PATHWAYS FOR THERMOLYSIS OF 9,10-DIMETHYL-ANTHRACENE.

P.S. Virk and V.J. Vlastnik
Department of Chemical Engineering, M.I.T., Cambridge, MA 02139.

Keywords: Reaction Paths, Pyrolysis, Kinetics, Demethylation

ABSTRACT. We report experiments on thermolysis of 9,10-dimethyl-anthracene (DMA) at temperatures from 315-409 C with initial concentrations from 0.1-3.0 M. Substrate conversions ranged from 0.05 to 0.98 with quantitative assays of major products. The substrate appears to decompose primarily by two parallel pathways, namely, demethylation (major) to 9-methyl-anthracene (MA) plus methane and disproportionation (minor) to MA plus tri-methyl-anthracenes (TMA). These reactions are also associated with hydrogen transfer, as inferred from the detection of 9,10-dihydro-9,10-dimethyl-anthracenes (DHDMA). At the higher substrate conversions, the primary reaction products appear to be secondarily operated upon by a parallel pathway pair analogous to the primary pair, eventually forming anthracene (ANT). Also, minor amounts of the 1- and 2-methyl-anthracenes (1MA, 2MA) were detected, both arising subsequent to the appearance of the parent acene. A preliminary mechanism is presented for DMA thermolysis, based on elementary free-radical and molecular reactions relevant to the present conditions, combined with the experimentally observed kinetics and product selectivities. Also, frontier-orbital theory is applied to model the observed 1MA and 2MA isomer distributions.

INTRODUCTION

The present work on DMA thermolysis is part of a continuing study of simple substrates that mimic the chemical moieties found in complex fossil materials of engineering interest. DMA was chosen for two reasons. First, its acene aromatic ring system is prototypical of the aromatic molecules found in fossil fuels, and its methyl moieties model the electron donating substituents commonly pendant on the aromatic rings of natural materials. Second, its thermal destruction is of environmental interest, the intermediate decomposition product, MA, being far more toxic than either the original DMA or the final ANT.

There appear to be no previous studies of DMA thermolysis in the literature, save for a preliminary investigation in our laboratories (Pope 1987) that is elaborated here. However, the literature does contain references to pyrolyses of the related MA (Pomerantz 1980) and ANT (Stein 1981) substrates.

In outline, we briefly describe the experimental approach and present representative results for the concentration histories and product selectivities observed during DMA thermolysis. Reaction pathways inferred from these results are then summarized, leading to a preliminary mechanism for the early stages of DMA thermolysis. Finally, frontier orbital theory is applied to understand the formation of certain minor methylated products.

EXPERIMENTAL

The chemicals used, DMA (Aldrich 99% purity), biphenyl (BIP) (Aldrich 99% purity) and methylene chloride (EM Science omnisolv), were all obtained commercially and used as received.

Pyrolyses were conducted in batch reactors, volume 0.49 ml, made from 1/4" stainless steel Swagelok parts. The reactors, purged with inert gas, were charged with weighed amounts of biphenyl (internal standard) and DMA substrate totalling 0.30 g, sealed, and placed in an isothermal, fluidized-sand, bath for the appropriate holding time, after which they were quenched in ice-water, and their contents extracted into methylene chloride. Based on their

melting and critical properties, the biphenyl and DMA reactor contents were in the liquid phase during all experiments.

Products were identified and assayed by an HP-5890 Series II Gas Chromatograph equipped with flame ionization (FID) and thermal conductivity (TCD) detectors and on-column and split/splitless injectors. Liquid products were analysed using on-column injection, a 25m HP-101 column, and the FID. Product concentrations were calculated from experimentally determined response factors, using biphenyl as internal standard. Identified compounds typically accounted for >90% of total product mass at low fractional substrate conversions, X < 0.4, but only about 70% of total product mass at the highest conversions, X > 0.8.

Figure 1 shows the experimental grid traversed, DMA being pyrolysed at initial concentrations from 0.1 to 3.0 M, temperatures between 315 and 409 C, and holding times from 450 to 28800 s.

RESULTS

Representative concentration histories obtained during DMA pyrolysis at T = 409 C and [DMA]o = 1.0 M are chronicled in Figure 2, with coordinates absolute mols of each identified compound, j, versus time, s. The plot clearly depicts the continuous decay of substrate DMA, the initial growth, maximum, and final decay exhibited by the primary product MA, and the initial absence and final growth of the secondary product ANT. The major thermolysis pathways evidently involve the demethylation sequence DMA → MA → ANT. Closer scrutiny reveals small amounts of TMA at low times, and the formation of methyl-anthracenes, with 1MA > 2MA. Also, though not seen in Figure 2, small amounts of DHDMA were clearly visible at lower temperatures. The minor thermolysis pathways thus involve methylations of both the DMA substrate and the ANT final product, as well as hydrogen transfers that lead to DHDMA.

Additional insights into the operative pathways are offered by the selectivity diagram in Figure 3, which shows the selectivity S(j), that is, (mols j formed/mol DMA reacted), versus conversion. For low X < 0.6, it is seen that both S(MA) ~ 0.5 and S(TMA) ~ 0.1 are essentially constant, implying that MA and TMA are both primary products of DMA thermolysis, resulting from parallel pathways that are respectively fast and slow. For high X > 0.6, the mirror-image decrease in S(MA) and increase in S(ANT) is evidence that ANT is a secondary product, arising from the primary product MA. Too, S(1MA) and S(2MA) are each essentially zero for X < 0.6, where S(MA) is large, and increase only for X > 0.6, when S(ANT) becomes appreciable. This timing implies that the 1MA and 2MA arise from methylation of ANT, and not from isomerization of MA.

PATHWAYS

Pathways for thermolysis of DMA, inferred from results over the entire experimental grid, are summarized in Figure 4. The main demethylation sequence, shown bold, cascades from DMA to MA to ANT. Compounds in the main sequence are all subject to methylation, forming the various methyl substituted anthracenes shown to the right, but neither MA nor DMA isomerize to their positional isomers. DMA is also hydrogenated to DHDMA (cis- and trans-isomers not distinguished). In overall, unbalanced, terms, based on detected products, the primary parallel reactions of DMA are:

(RO1)	Demethylation	fast	DMA → MA (+ CH4 + heavy products)
(RO2)	Disproportionation	slow	DMA → MA + TMA
(RO3)	Hydrogenation	slow	DMA → DHDMA

A similar set of three pathways presumably operates on MA, by analogy, but we have evidence only of the demethylation step, forming ANT.

Kinetic information was also derived from the experiments that delineated the DMA thermolysis pathways. At T = 355 C, initial conversion data for 0.1 < [DMA]o < 3.0 M suggested that the overall decomposition was ~3/2 order in DMA. For fixed [DMA]o = 1.0 M, initial conversion data at temperatures 315 < T < 409 C, showed an apparent activation energy ~55 kcal/mol.

MECHANISM

A possible mechanism for the early stages of DMA thermolysis, that is consistent with the present pathway and kinetic observations, is enumerated below and illustrated by the "Tolman clock" formalism in Figure 5. The elementary molecular and free-radical steps are:

Initiation		
(R1)	2DMA → HDMA• + DMA•	(Molecular disproportionation)
Propagation		
(R2)	HDMA• → CH3• + MA	(MA formation)
(R3)	CH3• + DMA → DMA• + CH4(g)	(H abstraction)
(R4)	CH3• + DMA → HTMA•	(CH3 addition)
(R5)	HTMA• + DMA → HDMA• + TMA	(TMA formation)
Termination		
(R6)	2 HDMA• → DHDMA + DMA	(Radical disproportionation)
(R7)	2 DMA• → DMAD	(Dimer formation)

The initiation reaction, (R1), involves H atom transfer from the methyl of one DMA molecule to the 9 position of another, forming the corresponding DMA• and HDMA• radicals. The propagation sequences involve two parallel clocks that respectively form either MA + CH4 (R2 + R3) or TMA + MA (R2 + R4 + R5); the latter slower than the former by the kinetic ratio R4/R3 ~ S(TMA)/S(MA) ~ 0.2. Of the termination steps, (R6), the disproportionation of chain-carrying HDMA• radicals, accounts for the observed DHDMA product. However, there is yet no independent evidence for (R7), the combination of DMA• radicals to form dimer, although unidentified heavy products do indeed arise.

Steady-state analysis of the preceding mechanism indicates that the observed reaction orders wrt [DMA] should respectively be 1 and 2 for terminations controlled by (R6) and (R7); these bracket the experimentally observed order of 3/2.

FRONTIER ORBITAL MODEL

The observed formations of 1MA and 2MA from ANT during DMA thermolysis at high severities invite interpretation according to frontier orbital theory, as examples of periselective methyl radical attack on the ANT nucleus. Following Fukui (1975), an interaction diagram for this system is shown in Figure 6. The corresponding expression for the FMO stabilization energy is given in the bottom line of the figure, using the coefficients and energies of the CH3 radical SOMO (singly-occupied MO) and the ANT HOMO and LUMO (highest occupied and lowest unoccupied MOs). The evaluation of these expressions is depicted graphically in Figure 7. Here each position on the ANT ring framework is decorated with its HOMO coefficients, Ct(HO), derived from MINDO calculations (Clark 1985, Dewar 1970), and then positions 9, 1, and 2 are shown interacting with the methyl radical SOMO, having Cu(SO) = 1. The resulting, favourable, nondimensional stabilization energy, denoted $\Delta E'$(FMO), is respectively 0.232 and 0.117 at positions 1 and 2 (position 9 is not in contention here). FMO theory thus predicts methyl radical attack favoured in the order position 1 >

position 2. The latter inequality accords with the experimental observation, from Figures 2 and 3, that 1MA > 2MA.

CONCLUSIONS

1. Thermal decomposition of DMA was experimentally studied at 0.1 < [DMA]o < 3.0 M, 315 < T < 409 C, covering fractional substrate conversions 0.05 < X < 0.98.
2. DMA decomposition pathways included:
(RO1) Demethylation fast DMA → MA (+ CH4 + heavy products)
(RO2) Disproportionation slow DMA → MA + TMA
(RO3) Hydrogenation slow DMA → DHDMA
3. The MA product decomposed by pathways analogous to DMA.
4. At low conversions, DMA decomposition was ~3/2 order in DMA, with apparent activation energy E* ~55 kcal/mol.
5. A mechanism was devised for DMA decomposition, comprizing 7 elementary steps. This acounted for the reaction products and kinetics observed at low DMA conversions.
6. Minor products 1MA and 2MA observed at high DMA conversions appeared to arise from ANT methylation rather than 9MA isomerization.
7. The relative amounts of 1MA and 2MA observed experimentally were interpreted by FMO theory, as periselective methyl radical additions.

REFERENCES

Clark, T.: "A Handbook of Computational Chemistry", Wiley, New York (1985).
Dewar, M.J.S.; Haselbach, E.; Worley, S.D.: *Proc. Roy. Soc. Lond.* **A315**, 431 (1970).
Fukui, K : "Theory of Orientation and Stereoselection", Springer-Verlag, Berlin (1975).
Pomerantz, M.; Combs, G.L.; Fink, R.: *J. Org. Chem.*, **45**, 143 (1980).
Pope, J.M.: Sc.D. Thesis, Dept. of Chem. Eng., MIT, Cambridge, MA (1987).
Stein, S.E.: *Carbon*, **19**, (6) 421 (1981).

FIGURES

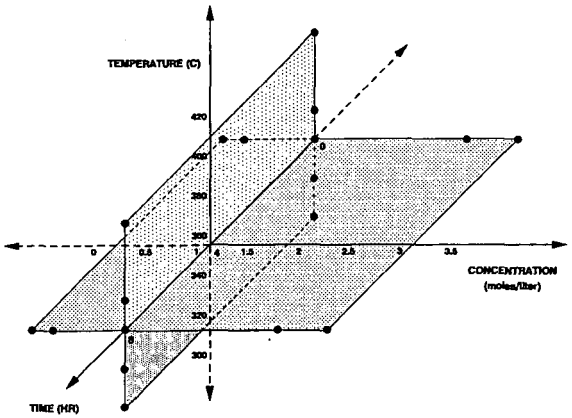

Figure 1. Experimental Grid.

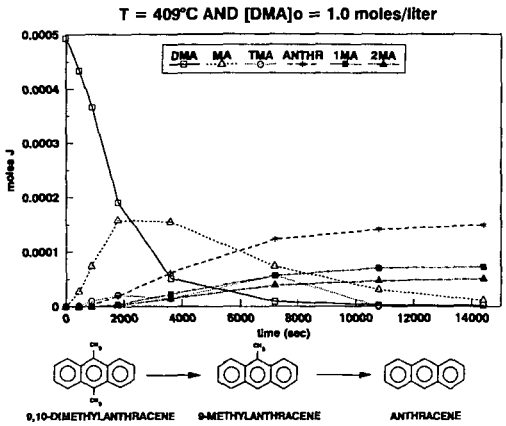

Figure 2. Concentration Histories.

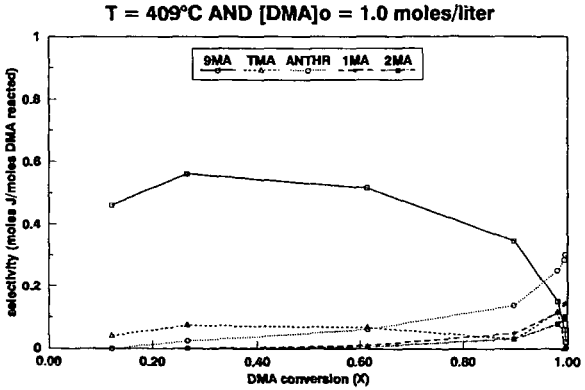

Figure 3. Selectivity Diagram.

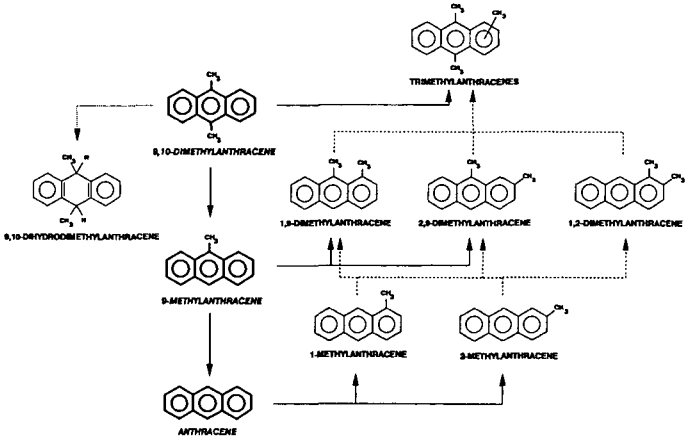

Figure 4. DMA Pyrolysis Pathways.

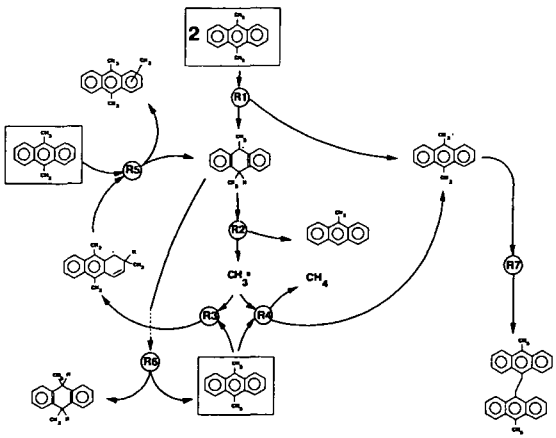

Figure 5. DMA Pyrolysis Mechanism.

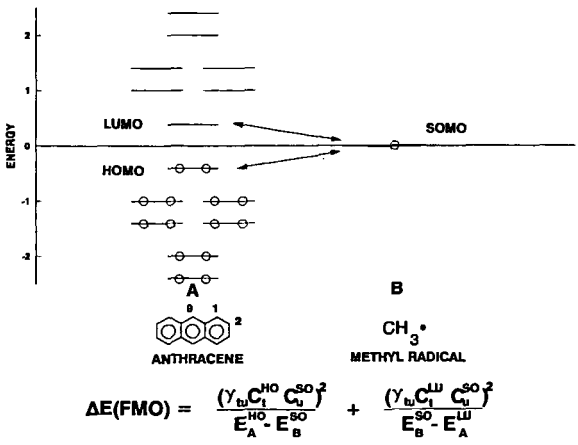

Figure 6. Frontier Orbital Interaction Diagram.

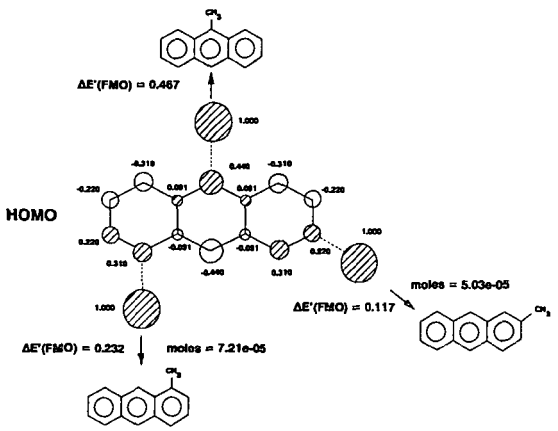

Figure 7. Periselectivity of Methyl-Anthracenes.